# Validation of URANS and LES Solutions in a Closed Rotor-Stator Disc Cavity

S. Kanjiyani, A.V. Mirzamoghadam
Advanced Technology
Honeywell Aerospace
111 S. 34th St.
Phoenix, AZ 85034

## Abstract

In gas turbines, the amount of cooling air assigned to seal high pressure turbine rim cavities is critical for performance as well as component life. Insufficient air leads to excessive hot annulus gas ingestion and its penetration deep into the cavity compromising disc or cover plate life. Excessive purge air, on the other hand, adversely affects performance. Therefore, considerable effort is being taken to improve disc cavity cooling technology including tool validation. The scope of this work is to validate the CFD tool by comparing its predictions against experimental LDV data in a closed rotor-stator cavity. The enclosed cavity has a stationary shroud, a rotating hub, and mass flow does not enter or exit the system. A full 360 degree numerical simulation is performed comparing Fluent LES, with unsteady RANS using Spalart-Allmaras, RNG k-ε, Realizable k-ε, Reynolds Stress, k-ω, and SST k-ω turbulence models. The goal of this task is to assess the validity of URANS turbulence models in more complex rotating flows, compare accuracy with LES simulations, and suggest CFD settings to better simulate turbine stage mainstream/disc cavity interaction with ingestion.

## Nomenclature

| | |
|---|---|
| a | hub radius, m |
| b | Radius to stator angle wing inner surface, m; shroud radius |
| Cw | Non-dimensional purge supply flow, $\frac{\dot{m}}{\mu b}$ |
| $C_{wmin}$ | Minimum value of Cw to prevent ingestion |
| Cp | specific heat at constant pressure, J/kg-k |
| f | body forces |
| $\dot{m}$ | Cavity purge/cooling supply flow (kg/s) |
| P | Pressure, N/m2 |
| r | radial coordinate, m |
| R | Shroud radius, m |
| Re | Rotational Reynolds number, $\frac{\rho\Omega b^2}{\mu}$ |
| T | Temperature, K |
| h | Axial spacing between rotor and stator; radial or axial gap, m |
| u | Velocity vector, m/s; |
| z | axial direction |

**Greek**

| | |
|---|---|
| ρ | Fluid density (kg/m3) |
| Ω | Angular velocity (rad/s) |
| τ | Stress tensor (N/ m2) |
| ø | tangential direction |
| μ | Fluid dynamic viscosity, kg/m-s |

**Subscripts**

| | |
|---|---|
| c | Concentration-based |
| h | Turbine cavity hub location |
| hub | Turbine cavity local property at hub location |
| max | Maximum |
| min | Minimum |
| t | Tangential; total property |
| z | Axial direction |

**Acronyms**

| | |
|---|---|
| RANS | Reynolds averaged Navier Stokes |
| URANS | Unsteady Reynolds averaged Navier Stokes |
| LES | Large Eddy-Simulations |

## Introduction

Rotating and swirling flows are one of the most complex phenomena in heat transfer and fluid mechanics, and they appear in many engineering and scientific applications such as jet engines, pumps, tip vortex on air-craft wings, tornadoes, geophysics and astrophysics [1]. The goal of this investigation is to better understand flow in rotor-stator disc cavities which are applicable to gas turbine engines.

The amount of cooling or secondary flow which is allocated from the compressor to cool the turbine section is one of driving factors in influencing efficiency of the system. In an effort to improve turbine efficiency, researchers and designers are always looking to reduce this cooling flow. One of these areas is the turbine stage mainstream/disc cavity interaction.

As shown in Figure 1, turbine stage mainstream/disc cavity is the complex interaction between hot annulus flow and cooler purge flow in the rotor-stator disc wheel space. Allocating insufficient purge flow would cause ingestion of the hot mainstream gas to travel inside the cavity, thus raising the metal temperatures of the stationary and rotating components. On the other hand, assigning excessive purge flow would degrade performance. In order to optimize purge flow, accurate CFD simulations of the turbine stage mainstream/disc cavity needs to be performed.

What makes the CFD difficult to simulate is that in the gas path there are pressure pulses resulting from the stator flow interacting with the rotor. In addition, these pressure pulses are interacting with the cavity where there is a rotating and a stationary disc. At low purge flow conditions, the vortices that form inside the cavities are greatly influenced by mainstream ingestion. Conversely at high purge flow conditions the vortices are influenced by the purge flow, therefore ingestion is minimized.

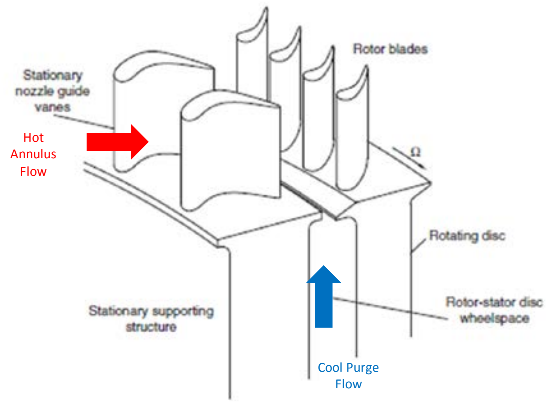


**Figure 1.** Turbine stage mainstream/disc cavity

This work is an extension of the work done previously in which an unsteady RANS (i.e. URANS), 360-degree CFD model of the complete turbine stage was employed in order to better predict rim seal ingestion in rotor-stator cavity [2]. One way to validate CFD predicted ingestion is by comparing the measured concentration based cavity effectiveness with CFD predicted cavity effectiveness, shown in Figure 2. It was found that both the simulation methodology and experimental validation can be improved. The slow response sealing effectiveness measurements do not adequately capture the fast response flow physics of ingestion. Additionally, it was not established that the CFD settings of the URANS Fluent model accurately predicts the fluid mechanics present in a rotating cavity. The CFD performed in the previous work shows the flow structure in the cavity is unstable circumferentially and still evolving after 16 revolutions. Furthermore, Craft [3] showed in his simulation of disc cavities using a two-equation turbulence model, that the flow does not reach steady state even after 70 revolutions. This provides one explanation on why the sealing effectiveness ($\eta_c$) does not match the data.

The objective of the work herein is to resolve the issue of choosing the correct CFD settings to accurately predict flows in a rotor-stator cavity with rim seal ingestion. Although, recently published experimental velocity data from ASU rig of a rotor-stator disc cavity with purge flow and ingestion exist ([4]), the CFD tool was first validated by comparing it against an isothermal closed rotor-stator cavity.

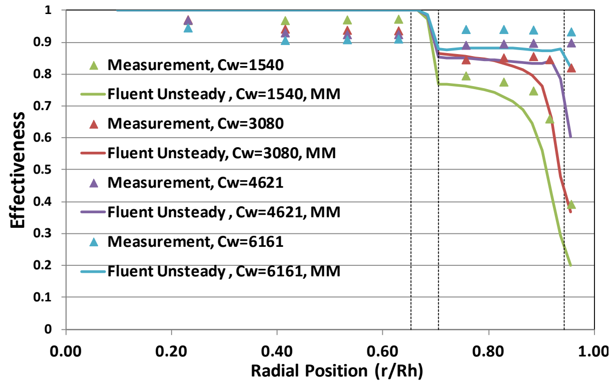


**Figure 2.** Sealing Effectiveness Comparison

The closed isothermal rotor-stator cavity has a stationary shroud, a rotating hub, and mass flow does not enter or exit the system as shown in Figure 3. If it can be shown for a rotor stator problem that numerical simulations agree with experimental results, this builds confidence that the same simulation settings gives useful results for the turbine stage mainstream/disc cavity problem without performing extensive CFD revalidation.

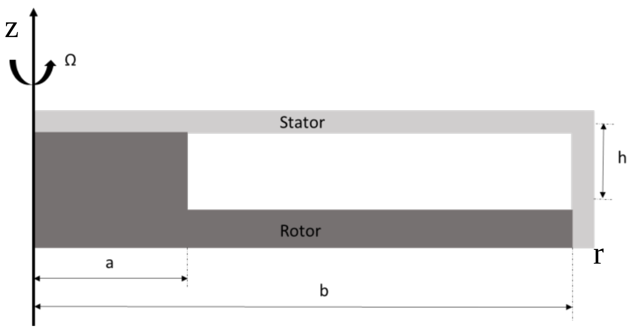


**Figure 3.** Enclosed Rotor-Stator Cavity [12]

## Previous Work

Using the closed rotor-stator cavity is an effective approach to understanding turbine stage mainstream/disc cavity. Before the advent of sophisticated CFD simulations, turbomachinery designers used theoretical and experimental studies performed on rotating disc systems in order to understand the fluid mechanics in the turbine stage disc. A brief summary of theoretical and experimental research on disc cavities spanning 1905-1988 follows. In 1905 Ekman [5] theoretically explained the formation of spirals in the outer layer of the ocean. Later Von Kármán [6] showed that for laminar flows over an infinite rotating disc, exact solutions for the Navier-Stokes equations can be found. He did this by simplifying the governing equations for a free disc assuming axisymmetric flow. This led to the understanding that the free disc pumps the fluid through the boundary layer forming radially over the disc. Von Kármán also showed turbulent solutions by using momentum integral methods with power law velocity profiles. After this, Batchelor [7] solved a case of two rotating discs of infinite radius. He observed that boundary layers formed on the surface of each disc, and confined between the boundary layers was a non-viscous core. Flow between a closed rotating and a stationary disc was described by Mellor [8]. In this case, a boundary layer forms on both the rotating and stationary disc; therefore the entire cavity is described by two boundary layers. The theoretical mass flow rate was also zero since the setup did not introduce mass flow into the system. Mellor also found that for the case of rotor-stator cavity the solution is not unique.

This was later confirmed by Daily and Nece [9] in 1960 who also performed experiments in closed rotor-stator cavities. They found the existence of four types of flows according to the rotational Reynolds number and the cavity non dimensional radial height. There are two laminar and two turbulent regimes. Bayley and Owen [10] performed experiments specifically related to turbomachinery shrouded disc cavities, and they determined the minimum gas sealing flow ($C_{w,min}$) to prevent main gas path ingestion was a function of non dimensional axial clearance (Gc) between the rotor and stator shroud and rotational Reynolds number ($Re_{\Omega}$). Phadke and Owen [11] tested seven sealing geometries, developed relations for $C_{w,min}$ for each geometry, and used flow visualization to observe main gas path ingestion flow structure. When compared to modern CFD simulations, these analytical and experimental techniques using simplified geometry seem outdated. But the advantage of a simplified geometry is that these simulations can quickly uncover incorrect modeling assumptions, and possible improvements to these assumptions can be verified in an efficient manner.

### Computational Details

The cavity shown in Figure 3 is composed of a stationary disc, rotating disc, inner rotating cylinder, and outer stationary shroud. The inner and outer disc radii are a=40 mm and b=140 mm, respectively; the inner disc spacing (h) is 20 mm, and Ω is the rotation rate. The rotational Reynolds number is based on the outer radius (b) on the disc. Séverac [12] performed experiments on this cavity where the fluid was water at 20 C. The experimental laser Doppler velocimetry (LDV) results obtained by Séverac can be used to compare with computational predictions.

The grid size for the 360 degree model and time steps for all numerical simulations are presented below in Table 1. It was observed for the simulation at Re=1E+05 that the solution remained numerically stable at 122.66 time steps per revolution of the rotating disc, and this parameter was maintained for all computational runs.

**Table 1.** Computational Parameters

| Computational Parameters | | | | | | |
|---|---|---|---|---|---|---|
| Re | Computation | Grid | | | time step (s) | time steps per rev |
| | | r | θ | z | | |
| 1.00E+05 | URANS/LES | 81 | 150 | 49 | 0.01 | 122.66 |
| 4.00E+05 | LES | 81 | 150 | 49 | 0.0025 | 122.66 |
| 1.00E+06 | LES | 81 | 150 | 49 | 0.001 | 122.66 |

The computations started with the fluid at rest. No-slip boundary conditions are applied on all cavity walls where $V_r$ and $V_z$ are zero. $V_\theta$=rΩ is applied on the rotor and hub, and is zero on all other walls.

For rotational Reynolds Number=1E+05, simulations of the closed rotor-stator cavity were performed using Fluent employing unsteady k-ω, k- ε, Spalart-Allmaras, RNG k- ε, Realizable k- ε, Reynolds Stress, and SST k-ω turbulence models. Additionally, a simulation was performed with LES (Smagorinsky-Lily Sub-Grid Scale (SGS) model). These computational results were compared with experimental data.

## Results

In the following results, the inner disc spacing has been normalized by h=20mm, therefore the non-dimensional axial spacing varies from 0-1. Both the radial and tangential velocity components are measured at mid-radius and these components are normalized by the maximum rotational velocity of the system; Vr'= $V_r$/rΩ and Vt'= $V_{t'}$/rΩ. The circumferential average location was taken for the velocity components mentioned above after 22 seconds of simulation.

It can be seen by the measured data below that flow inside the cavity is dominated by tangential velocity. The largest radial velocity component is 15% of the largest tangential velocity component. Data comparison with the tangential velocity is shown in Figure 4. The URANS simulations fail to capture the mean tangential velocity near the rotor, stator and the mid axial plane of the cavity. The URANS prediction at the mid axial plane range from 0.20-0.24, but the measured value is near 0.35. On the other hand, the LES simulation captures the mean tangential velocity at all locations. The URANS simulations shown in Figure 5 do however, capture the mean radial velocity near the rotor and the mid axial plane of the cavity, but near the stator, they fail to match the experimental data. It is expected that the minimum radial velocity should approach -0.15 whose minimum occurs between two measured data points, thus, it is not captured by the experiment. The minimum radial velocity at the stator location predicted by URANS is about -0.08. Conversely, the LES simulation captures the mean radial velocity near the rotor, stator and the mid axial plane of the cavity.

Based on the results discussed above the velocity profiles predicted by the LES model more closely resemble the LDV data.

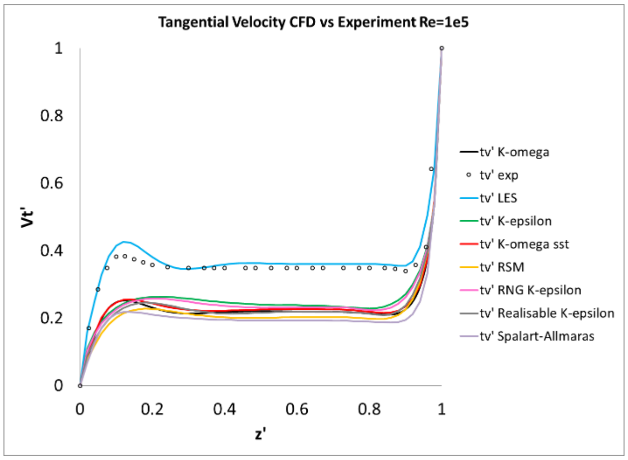


**Figure 4.** Tangential Velocity CFD vs Experiment Re=1E+05

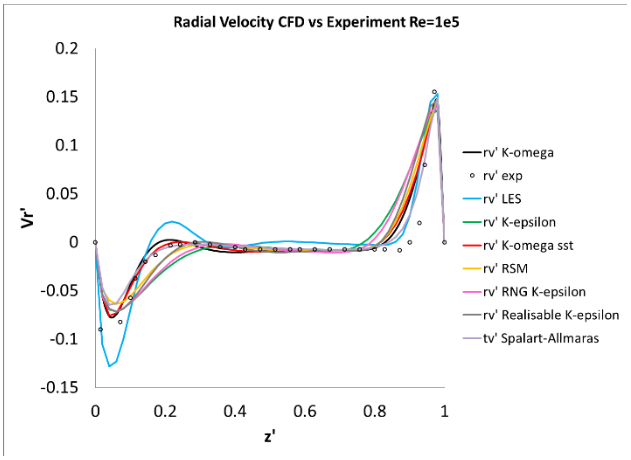


**Figure 5.** Radial Velocity CFD vs Experiment Re=1E+05

The LES model was further validated in Figures 6-9 where the numerical predictions were compared with experiments at Re=4E+05 and Re=1E+06. Similar to the previous data, the radial and tangential velocity components are measured at mid-radius. The circumferential average was taken for the velocity components mentioned above after 22 seconds of simulation.

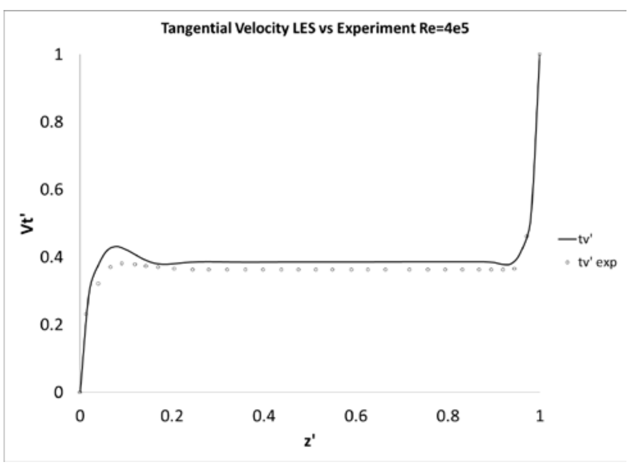


**Figure 6.** Tangential Velocity CFD vs Experiment Re=4E+05

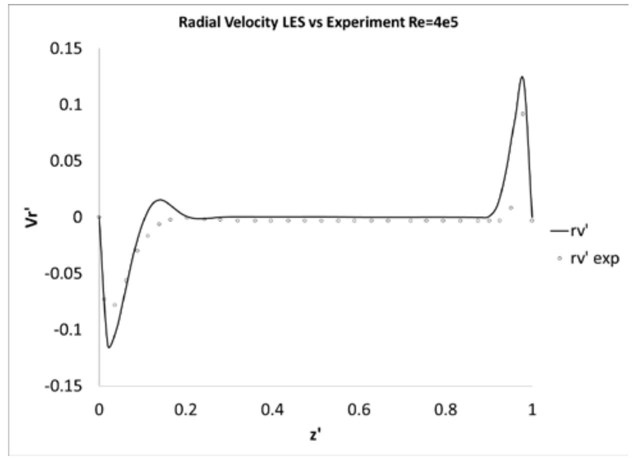


**Figure 7.** Radial Velocity CFD vs Experiment Re=4E+05

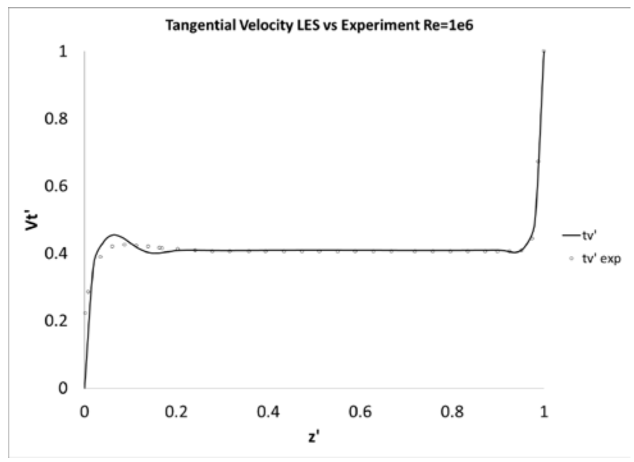


**Figure 8.** Tangential Velocity from CFD vs Experiment at Re=1E+06

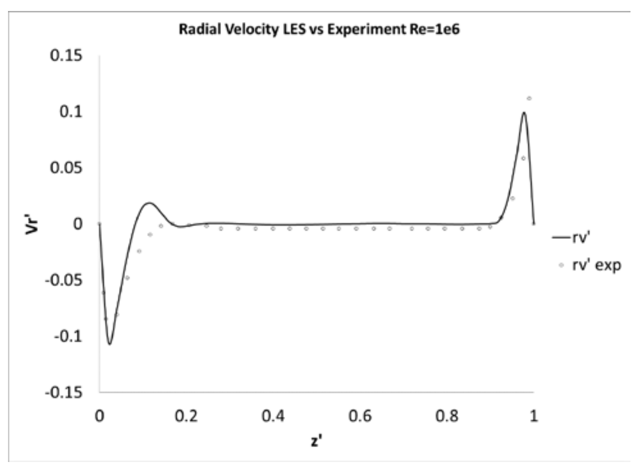


**Figure 9.** Radial Velocity CFD vs Experiment Re=1E+06

It can be seen that as the rotational Reynolds number increases, the dominance of the flow by tangential velocity is larger. The largest radial velocity component is about 12% of the largest tangential velocity component at Re=4E+05 and about 10% at Re=1E+06. This trend is captured by the LES model and additionally the model also matched the LDV data near the rotor, stator and the mid axial plane of the cavity at the higher Reynolds numbers, thereby confirming that in a rotating flow environment, LES simulations were accurately able to predict the radial and tangential velocities.

## URANS vs. LES, a Physics View-Point

In the numerical studies shown above LES has performed better in simulating flows in a closed rotating cavity when compared against URANS solutions. Although URANS solves the transient solution, it is unable to capture the temporal and spatial variation [13]. This is because in URANS simulations, the flow properties are organized into their mean and fluctuating components, and integration over time is performed. The continuity and momentum equations describing this process are:

$$\frac{\partial \bar{u}_i}{\partial x_i} = 0 \qquad (1)$$

$$\frac{\partial \bar{u}_i}{\partial t} + \bar{u}_j \frac{\partial \bar{u}_i}{\partial x_j} = -\frac{1}{\rho}\frac{\partial \bar{p}}{\partial x_i} + \nu \frac{\partial^2 \bar{u}_i}{\partial x_j^2} - \frac{\partial R_{ij}}{\partial x_j} \qquad (2)$$

Where, $R_{ij}$ is the Reynolds stress tensor which closes the governing equations by modeling the unknowns introduced by the averaging procedure. Therefore, URANS first captures the large scale fluctuations, and then it models fluctuations of the turbulent inertial and dissipation range. The LES equations are shown below:

$$\frac{\partial \bar{u}_i}{\partial x_i} = 0 \qquad (3)$$

$$\frac{\partial \bar{u}_i}{\partial t} + \bar{u}_j \frac{\partial \bar{u}_i}{\partial x_j} = -\frac{1}{\rho}\frac{\partial \bar{p}}{\partial x_i} + \nu \frac{\partial^2 \bar{u}_i}{\partial x_j^2} - \frac{\partial \tau_{ij}}{\partial x_j} \qquad (4)$$

Although, the LES equations are similar to the RANS equations, in LES the over-bar designates spatial filtering. The filter is a function of grid size, and turbulent scales smaller than the grid size are removed and modeled by a sub-grid scale defined as $\tau_{ij}$. This means that eddies larger than the grid size are solved numerically by the filtered N-S equations. Therefore fluctuations of the flow field that transfer momentum at the smaller scales are captured by the LES equations. These fluctuations are important to model turbulent rotating flows, and thus, the velocity profiles predicted by the LES models more closely resemble the LDV data.

## Conclusions

Two different CFD techniques, URANS and LES simulations were validated in a closed rotor stator cavity to offer CFD settings for better turbine stage mainstream/disc cavity ingestion predictions. It was shown in a closed rotating cavity that in order to accurately predict rotating flows, it is imperative to model the small scale fluctuations. URANS is unable to account for these fluctuations in the flow field, as its accuracy is limited to large scale structures. Therefore, the under predicting of cavity sealing effectiveness compared to the data (see Fig. 2) in the URANS simulations of turbine stage mainstream/disc cavity is by extension from this study allocated to the limitation of URANS. LES matched experimental data of the velocity profiles in an enclosed rotor-stator cavity because it resolves these small scale structures. Therefore, LES simulation is recommended to accurately predict turbine stage mainstream/disc cavity sealing effectiveness in addition to the velocity field observed here. The validity of this recommendation will be a subject of a future paper.

## REFERENCES


[1] Peter R. N. Childs. (2010). Rotating Flow. London: Butterworth-Heinemann.

[2] Mirzamoghadam, A.V., Kanjiyani, S., Riahi, A., Vishnumolakala, R., and Gundeti, L., (2014), "Unsteady 360 CFD Validation of a Turbine Stage Mainstream/Disc Cavity Interaction", ASME GT2014-25466, Journal of Turbomachinery 01/2015.

[3] Craft, T., Iacovides, H., Launder, B., & Zacharos, A. (2008). Some swirling-flow challenges for turbulent CFD. Flow, Turbulence and Combustion, 80(4), 419-434.

[4] Dunn, D.M, Zhou, D.W., Saha, K., Squires, K.D., Roy, R.P., Kim, Y.W., and Moon, H.K. (2010), "Flow Field in a Single-Stage Model Air Turbine Rotor-Stator Cavity with Pre-Swirled Purge Flow", ASME GT2010-22869.

[5] Ekman, V.W. (1905), On the influence of the Earth's rotation on ocean-currents. Arkiv. Mat. Astr. Fys., 2(11):1-52.

[6] Von Kármán, T. (1921), "Uber laminare und turbulente Reibung", Z. Angew. Math. Mech., 1:233-252.

[7] Batchelor, G. K. (1951). Note on a class of solutions of the Navier-Stokes equations representing steady rotationally-symmetric flow. The Quarterly Journal of Mechanics and Applied Mathematics, 4(1), 29-41.

[8] Mellor, G. L., Chapple, P. J., & Stokes, V. K. (1968), On the flow between a rotating and a stationary disc. J. Fluid Mech, 31(1), 95-112.

[9] Daily, J. W., & Nece, R. E. (1960), Chamber dimension effects on induced flow and frictional resistance of enclosed rotating discs. Journal of Basic Engineering, 82, 217.

[10] Bayley, F. J., & Owen, J. M. (1970), The fluid dynamics of a shrouded disc system with a radial outflow of coolant. Journal of Engineering for Power, 92(3), 335.

[11] Phadke, UP, and Owen, J.M (1988), "Aerodynamic Aspects of the Sealing of Gas Turbine Rotor-Stator Systems, Part 1: The behavior of simple shrouded rotating-disc systems in a quiescent environment, vol. 9, pp.98-105.

[12] Éric Séverac, et al. "Large Eddy Simulation and Measurements of Turbulent Enclosed Rotor-Stator Flows." Physics of Fluids 19.8 (2007):

[13] ANSYS. ANSYS Fluent Theory Guide. ANSYS Fluent; 2011.